LIFE-TIME ENGINEERING ASSESSMENT FRAMEWORK FOR FLOATING OFFSHORE WIND FARMS

Heng Zhu
Chalmers University of Technology
Department of Mechanical Engineering
Division of Marine Technology
Gothenburg, Sweden

Xinyuan Shao
Chalmers University of Technology
Department of Mechanical Engineering
Division of Marine Technology
Gothenburg, Sweden

Shan Wang
Instituto Superior Técnico
Centre for Marine Technology and Ocean Engineering
Lisbon, Portugal

Jonas W. Ringsberg
Chalmers University of Technology
Department of Mechanical Engineering
Division of Marine Technology
Gothenburg, Sweden

ABSTRACT

Floating offshore wind farms (FOWFs) offer access to high-quality wind resources in deep-water regions, but their large-scale deployment is constrained by high costs and uncertainties in long-term performance and environmental impact. To support early-stage design decisions, this study aims to develop an integrated life-time engineering (LTE) framework that combines life-cycle cost (LCC), life-cycle assessment (LCA), and life-cycle performance (LCP) considerations within a numerical platform. The modular framework is implemented in MATLAB Simulink and OpenLCA, allowing targeted analysis of critical components. In this paper, particular emphasis is placed on the mooring system, which represents a major contributor to capital expenditure. The LCC and LCA models are formulated with consistent system boundaries and inventories, allowing material- and configuration-driven trade-offs to be evaluated in a coherent manner. Case studies are conducted for spar and semi-submersible floating platforms equipped with alternative mooring line configurations, including all-chain and chain-polyester-chain systems, focusing on manufacturing-stage costs and environmental impacts. The results suggest that the integrated LTE framework can support identifying coupled cost-environmental trade-offs that are not accessible through isolated assessments. By providing a flexible and extensible tool for comparative analysis, the proposed methodology supports decision-making for the design and optimization of mooring systems in FOWFs.

Keywords: floating offshore wind; life-cycle assessment; life-cycle cost; life-time engineering; mooring systems.

NOMENCLATURE

C_1	Concept and definition cost [€]
C_2	Design and development cost [€]
C_3	Manufacturing cost [€]
C_{31}	Manufacturing cost of OWTs [€]
C_{32}	Manufacturing cost of floating platforms [€]
C_{33}	Manufacturing cost of mooring [€]
C_{331}	Manufacturing cost of mooring for floating platforms [€]
C_{332}	Manufacturing cost of substation mooring [€]
C_{34}	Manufacturing cost of anchoring [€]
C_{35}	Manufacturing cost of electric systems [€]
C_4	Installation cost [€]
C_5	Exploitation cost [€]
C_6	Dismantling cost [€]
$CF_{\mathrm{CO_2}-eq}$	Characterization factor of $\mathrm{CO_2}$-eq [-]
CF_k	Characterization factor of category k [-]
C_{power}	Cost of power ratio [€/MW]
C_{total}	Total LCC [€]
E_i	Environmental load of component i [kg $\mathrm{CO_2}$-eq]
E_t	Expense on year t [€]
f_{ij}	Quantity of component i, flow j [kg]
GWP_{100}	Global warming potential [kg $\mathrm{CO_2}$-eq]
$LCoE$	Levelized cost of energy [€/MWh]
L_{moor}	Length of mooring line [m]
N_{ml}	Number of mooring lines per FOWT [-]
N_{wt}	Number of FOWTs [-]

r	Discount rate [-]
uC_{moor}	Cost per kg of mooring lines [€/kg]
uM_{moor}	Mass per meter of mooring lines [kg/m]
t_{farm}	Total life-cycle year [year]
α_j	LCI coefficient for flow j [-]

1. INTRODUCTION

The global transition towards sustainable energy is heavily reliant on expanding renewable capacity, where floating offshore wind turbine (FOWT) technology presents a significant opportunity for harvesting wind resources in deep waters. Industry forecasts suggest that floating offshore wind could contribute over 260 GW of global capacity by 2050 [1], yet its commercial viability depends on substantial cost reductions. For instance, initiatives, such as the U.S. Floating Offshore Wind Shot, aim to reduce the levelized cost of energy (LCoE) to \$45/MWh by 2035, representing a reduction of over 70% from current baselines [2]. Achieving these ambitious targets requires not only cost-effective engineering but also ensuring long-term structural integrity and minimal environmental impact. However, traditional design approaches often treat techno-economic, environmental, and structural performance analyses as separate domains, leading to sub-optimal designs and missed opportunities for integrated system-level optimization.

To address this challenge, a comprehensive methodological approach known as life-time engineering (LTE) is required. LTE systematically evaluates the economic, environmental, and structural performance of engineered systems across their entire life cycle, encompassing material extraction, manufacturing, installation, operation, maintenance (O&M), and decommissioning [3-5]. This framework integrates three interdependent pillars: life-cycle costing (LCC), which quantifies long-term economic performance and directly informs LCoE; life-cycle assessment (LCA), which evaluates environmental impacts in accordance with ISO 14040/44 standards [6]; and life-cycle performance (LCP), which assesses structural integrity, functional reliability, and degradation mechanisms throughout the operational lifetime.

Meanwhile, for FOWTs, the mooring and anchoring system represents a critical subsystem from both economic and structural perspectives, accounting for approximately 15–25% of the total capital expenditure (CAPEX) [5, 7]. In recent years, shared mooring concepts have attracted increasing attention due to their potential to reduce material usage and installation effort, with reported CAPEX savings of 15 – 35% compared to conventional individual mooring configurations [5, 7-9]. However, shared mooring systems also introduce new engineering challenges, including increased dynamic coupling between turbines, altered mooring fatigue loading patterns, and more complex failure and redundancy characteristics [10]. These challenges are further compounded by the growing adoption of synthetic fiber ropes, such as polyester, whose non-linear viscoelastic behavior influences both structural performance and long-term maintenance requirements [7, 11, 12].

Although significant progress has been made in the separate development of LCC, LCA, and LCP methods for FOWTs, existing studies often lack a fully integrated and holistic framework capable of consistently capturing the interactions between economic, environmental, and structural performance, particularly for novel mooring configurations and materials, applied to FOWT park installations. For example, the use of synthetic polyester fiber ropes, which are central to modern deep-water mooring design, introduces non-linear viscoelastic performance that must be accurately modelled within LCP to inform reliable maintenance and replacement schedules, thereby directly contributing to LCC and LCA [13]. Generic assumptions and limited public data further complicate the assessment of real-world trade-offs, especially for early-stage design decisions where uncertainties are high.

This paper presents an integrated LTE framework being developed within the ESOMOOR project, an EU-funded initiative aimed at advancing shared mooring system design for floating offshore wind farms. The proposed framework links component-level LCC implemented in a MATLAB Simulink environment with high-resolution LCA using OpenLCA, complemented by an LCP strategy for structural performance evaluation. The framework is designed to be modular and extensible, enabling systematic comparison of design alternatives at an early design stage. Case studies are presented for spar and semi-submersible floating platforms equipped with different mooring line configurations, including all-chain and chain-polyester-chain systems, focusing on manufacturing-stage economic and environmental impacts. The results suggest how integrated LTE assessment can support decision-making by revealing coupled cost-performance-sustainability trade-offs that are not accessible through isolated analyses.

2. METHODOLOGY

2.1 LCC model

The LCC model developed in this study aims to quantify the economic performance of floating offshore wind farm (FOWF) designs. The LCC framework is implemented for flexible configuration and systematic comparison of alternative design options at an early design stage.

LCC framework and cost breakdown

The LCC framework is divided into three modules: data input, LCC calculation, and output metric calculation. The data input module collects design parameters and cost information from industrial partners and open databases. The LCC calculation module quantifies the economic performance of the FOWF by aggregating costs across six life-cycle phases [14-16]: concept and definition (C_1), design and development (C_2), manufacturing (C_3), installation (C_4), exploitation (C_5), and dismantling (C_6). The total life-cycle cost (C_{total}) is defined by Equation (1). Figure 1 shows the life-cycle phases of FOWTs.

$$C_{total} = C_1 + C_2 + C_3 + C_4 + C_5 + C_6 \quad (1)$$

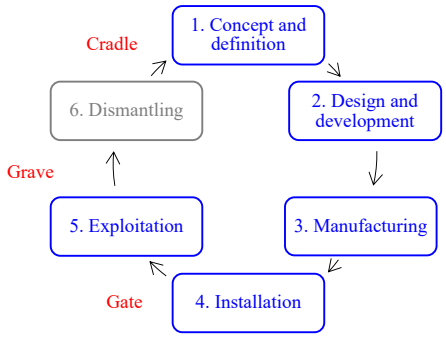

Figure 1: FOWT LIFE-CYCLE PHASES.

At the system level, the total cost of an FOWF is decomposed into contributions from offshore wind turbines (OWTs), floating platforms, mooring and anchoring systems, and electrical infrastructure, as shown in Figure 2. For example, the total cost of the manufacturing phase (C_3), is calculated by Equation (2), where C_1–C_5 represent the cost of each FOWT component, respectively. In this context, the detailed classification of the cost categories is presented in Figure 3.

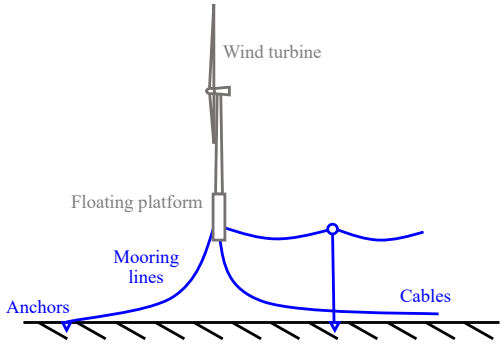

Figure 2: FOWT COMPONENTS.

$$C_3 = C_{31} + C_{32} + C_{33} + C_{34} + C_{35} \quad (2)$$

To support techno-economic comparison and decision-making, the LCC framework provides several commonly used economic indicators, i.e., the output metric calculation module. In addition to C_{total}, other economic performance metrics are calculated for analysis, including net present value (NPV), internal rate of return (IRR), discounted payback period ($DPBP$), $LCoE$, and cost of power ratio (C_{power}). For instance, the LCoE is computed by Equation (3), where C_{total_t} is the total life-cycle cost of the project in the period from year 1 to t_{farm}, E_t is the expenses on year t, and r is the discount rate. This formulation ensures consistency with broader project objectives and enables future extension of the analysis to full life-cycle evaluation.

$$\mathrm{LCoE} = \frac{\sum_{t=0}^{t_{farm}} \frac{C_{total_t}}{(1+r)^t}}{\sum_{t=0}^{t_{farm}} \frac{E_t}{(1+r)^t}} \quad (3)$$

Mooring line manufacturing cost modelling

In this paper, the case studies, which are presented in Section 3 in detail, are designed to highlight the cost sensitivity and trade-offs associated with alternative mooring concepts and materials. Therefore, mooring-related cost components are reported and discussed in greater detail, though the developed framework supports full cradle-to-grave life-cycle evaluation.

The manufacturing cost (C_3) is computed via component-specific breakdowns. For the mooring system, the cost (C_{33}) includes the manufacturing cost of the mooring lines for the FOWTs (C_{331}) and the substation platforms (C_{332}), i.e., Equation (4). C_{331} aggregates material and fabrication expenses for all line segments (*e.g.*, studless chain, stud-link chain, or polyester rope), as Equation (5) presents, where uM_{moor} is the mass per

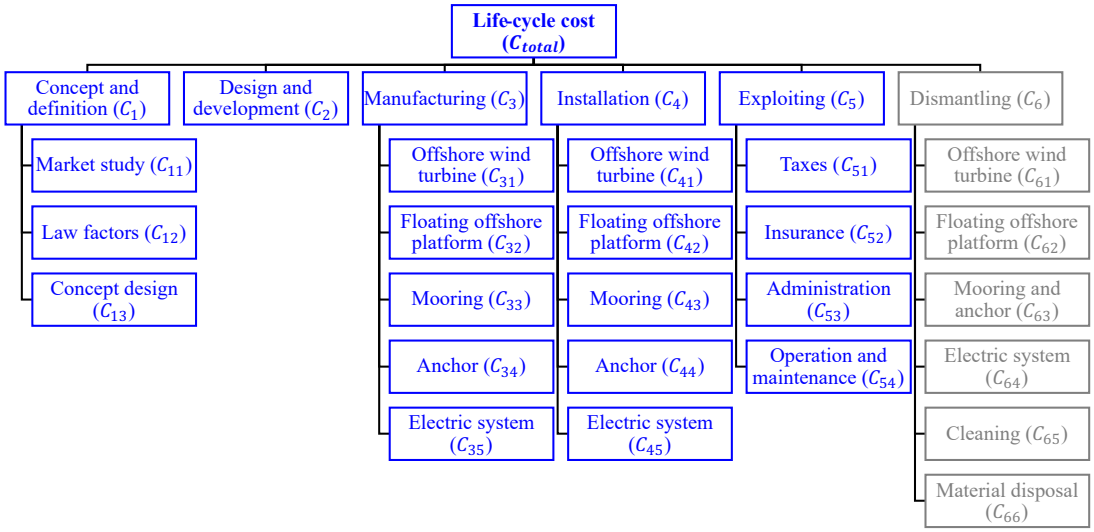

Figure 3: FOWT LIFE-CYCLE COST CATEGORIES.

meter of the mooring lines, L_{moor} is the length of the mooring lines, uC_{moor} is the cost per kg of mooring lines, N_{ml} is the number of mooring lines per FOWT, and N_{wt} is the number of FOWTs.

$$C_{33} = C_{331} + C_{332} \tag{4}$$

$$C_{331} = \sum(uM_{moor} \cdot L_{moor} \cdot uC_{moor} \cdot N_{ml} \cdot N_{wt}) \tag{5}$$

For synthetic fiber rope segments, the cost model explicitly accounts for rope diameter, material type, and construction, reflecting the strong dependence of cost on axial capacity and stiffness requirements. Compared to chain segments, fiber ropes typically exhibit lower mass per unit length, which has implications not only for manufacturing cost but also for installation logistics; however, installation-related effects are treated separately in the LCC framework and are not emphasized in the present manufacturing-stage analysis.

The total mooring system cost for a floating platform is obtained by aggregating the costs of all mooring lines connected to the platform, accounting for the number of lines per unit and, in the case of shared mooring configurations, the number of turbines sharing individual lines or anchors. This formulation enables direct comparison between conventional individual mooring systems and shared mooring concepts within a consistent cost framework.

Model implementation based on MATLAB Simulink

The LCC model is implemented as a modular and extensible MATLAB Simulink library. The objective of the library is to translate the analytical cost equations into reusable computational blocks that can be combined to evaluate LCC for different FOWF configurations, mooring concepts, and material systems.

The library follows the hierarchical structure of the LCC methodology by organizing components as divided in Figure 3. Each life-cycle phase is represented by a dedicated Simulink subsystem that integrates all corresponding input parameters, cost coefficients, and calculation routines. For instance, Figure 4 illustrates the structure of the LCC for the manufacturing phase in MATLAB Simulink.

2.2 LCA model

The objective of the LCA is to evaluate the environmental impacts of FOWT systems over their lifecycle. This assessment supports the identification of environmental hotspots and guides the selection of materials, components, and logistics strategies.

The LCA methodology follows the ISO 14040/44 standards [6, 17] and is implemented using OpenLCA [18], an open-source platform that support transparent and reproducible environmental assessment. The LCA model established in this study focuses on the cradle-to-grave environmental impacts of FOWT mooring, anchoring, and electrical systems, with particular emphasis on comparing different mooring materials, such as studless chains, stud link chains, polyester ropes, and nylon ropes, as well as dynamic power cable configurations. The LCA framework is structured around four main steps: goal and scope definition, life-cycle inventory (LCI), life-cycle impact assessment (LCIA), and interpretation.

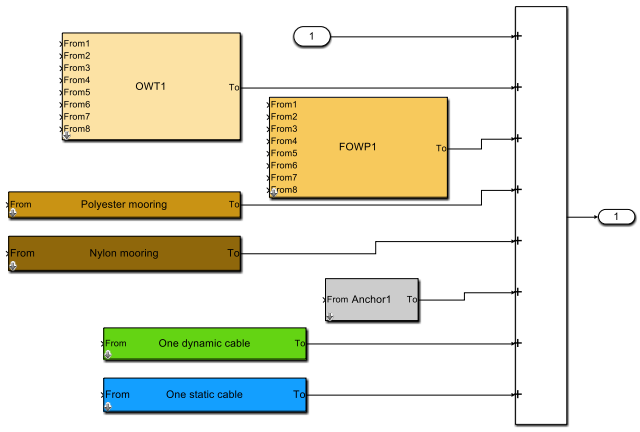

Figure 4: MODULAR IMPLEMENTATION OF THE LCC FOR THE MANUFACTURING PHASE IN MATLAB SIMULINK. FOWP PRESENTS THE FLOATING PLATFORM.

In the LCI phase, mass and material flows are quantified for each component category, including mooring lines, anchors, and dynamic and static cables. For a component i, its total environmental load (E_i) is computed as the sum of all contributing flows multiplied by their corresponding emission factors, i.e., Equation (6), where f_{ij} represents the quantity of flow j (*e.g.*, kg of steel, MJ of electricity, km of transportation), and α_j denotes the LCI coefficient for that flow.

$$E_i = \sum_{j=1}^{n}\left(f_{ij} \cdot \alpha_j\right) \tag{6}$$

The implementation in OpenLCA ensures that inventory data obtained from industrial partners, public databases (*e.g.*, ecoinvent), and design outputs can be incorporated consistently into the assessment. These inventory results are imported into OpenLCA and assigned to corresponding processes representing each subsystem of the mooring and cable assemblies. This modular representation is in parallel with the LCC Simulink structure described in Section 2.1, enabling one-to-one mapping between economic and environmental models.

The LCIA phase converts inventory flows into environmental impact indicators through characterization modelling. When assessing global warming potential (GWP_{100}), OpenLCA applies characterization factors (CF_k) derived from the chosen LCIA method (*e.g.*, CML-IA baseline [19], which is used in the case studies presented in Section 3). For each impact category k, the total environmental impact of the system is computed as Equation (7). Specifically, for GWP_{100}, it is simplified to Equation (8).

$$Impact_k = \sum_{i=1}^{m}(E_i \cdot CF_k) \tag{7}$$

$$GWP_{100} = \sum_{i=1}^{m}\left(E_i \cdot CF_{\mathrm{CO_2}-eq}\right) \tag{8}$$

This formulation supports consistent comparison of alternative design configurations by quantifying their total climate impact on the same basis. The OpenLCA implementation

also supports sensitivity analyses by allowing scenario-based modifications of input datasets, for example, substituting steel with low-carbon steel, varying recycling rates for metals or polymers, or evaluating alternative transportation routes and manufacturing origins.

2.3 LCP and LTE coupling strategy

Within the proposed LTE framework, LCP provides a structural and physical basis that constrains and informs both LCC and LCA. This role of LCP as the performance-driven foundation of the LTE framework is schematically illustrated in Figure 5. In contrast to the LCC and LCA components, which are implemented as quantitative models in the present study, the LCP model and the full LTE coupling implementation are under active development in the EU-funded ESOMOOR project. Therefore, LCP is introduced here at the level of a coupling strategy rather than as a standalone numerical model when establishing the LTE.

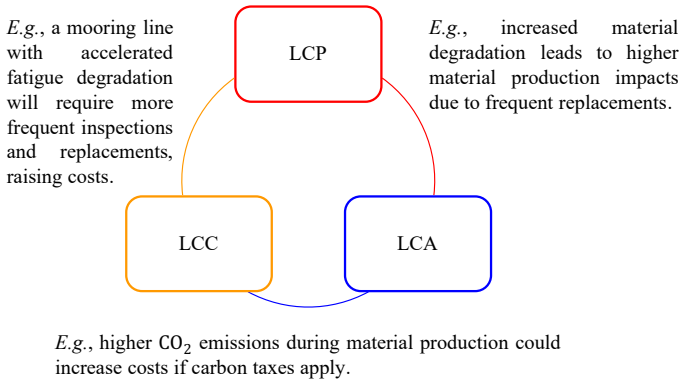

Figure 5: SCHEMATIC OVERVIEW OF THE INTEGRATED LTE FRAMEWORK ILLUSTRATING THE COUPLING BETWEEN LCP, LCC, AND LCA.

For FOWFs, LCP deals with structural integrity, functional reliability, and degradation mechanisms of key subsystems [20-25]. In this study, particular attention is given to the mooring system, where performance considerations such as strength requirements, fatigue resistance, and material behavior influence design parameters, including line diameter, material selection, and configuration. These performance-driven parameters define the admissible design space and serve as shared inputs within the LTE framework, ensuring that both LCC and LCA evaluations are performed consistently.

The coupling between LCP and LCC is formulated conceptually by translating structural performance requirements into cost-relevant parameters. For example, minimum strength and fatigue criteria determine material quantities and component specifications, which directly affect manufacturing costs. In extended applications of the LTE framework, LCP outputs are intended to inform O&M strategies and component replacement schedules. A similar coupling logic applies between LCP and LCA, where performance constraints influence material mass, composition, and assumed service life in the life-cycle inventory. As summarized in Figure 5, this coupling strategy follows a structured information flow in which LCP-derived performance constraints are transferred through a unified system interface to both the LCC and LCA modules. Aiming for consistent interaction among the three pillars, the LTE framework adopts a modular coupling strategy in which LCP-derived parameters are designed to be shared with the LCC and LCA modules through a unified system interface. This strategy establishes a clear pathway for future integration of quantitative LCP models while retaining flexibility for early-stage design exploration.

3. CASE STUDY RESULTS AND DISCUSSION

To demonstrate the practical application of the proposed LTE framework, a case study was conducted on two representative FOWT concepts: a spar-buoy platform and a semi-submersible platform [26, 27]. These two designs are widely deployed in deep-water wind farms and rely on taut or semi-taut mooring systems for station keeping. In this initial stage of the LTE framework development, the case study focuses specifically on the manufacturing phase of the mooring system, which serves as a controlled and well-defined subsystem for testing the LCC and LCA modules. The configurations analyzed provide a functional and consistent dataset for evaluating the current implementation of the cost and environmental assessment tools. Two deployment scenarios with water depths of 243.3 m and 799.2 m are selected to reflect typical European offshore sites and to examine the influence of water depth on mooring system characteristics.

The mooring system is modelled using a simplified three-segment representation, which reflects common engineering practice while allowing transparent comparison between configurations. Segment 1 (upper section) and Segment 3 (lower section) use the same material for each design variant, either studless chain or stud link chain, depending on the configuration. Segment 2, corresponding to the middle section, is assumed to use polyester rope. This setup aligns with industry trends toward hybrid mooring systems that reduce overall line weight in deep-water applications. All the mooring configurations are established using the quasi-static analysis procedure [28].

The LCC assessment follows the methodology described in Section 2.1. All cost calculations are performed using a self-developed MATLAB tool, which includes a Simulink-based visualization of the cost modules. The design parameters for each mooring configuration, including line lengths, diameters, materials and anchor characteristics, are based on the recorded design basis [26, 27]. Cost information for the materials, the manufacturing and the installation is provided by Bekaert nv-sa (Belgium) and Bexco nv-sa (Belgium) through direct industrial communication and is therefore treated as confidential industrial input data. In addition, the cost information is complemented with publicly available data from the literature and commercial sources [16, 29, 30].

The LCA follows the procedure outlined in Section 2.2, and the modelling is conducted using the open-source platform OpenLCA. The ELCD (European Reference Life Cycle Database) is used as the primary background database, and default providers are considered for all material and energy

processes. Environmental impacts are quantified using the CML-IA baseline method [19], which covers midpoint indicators such as global warming potential, acidification, eutrophication and abiotic depletion. Figure 6 shows an example of the material input flow in OpenLCA.

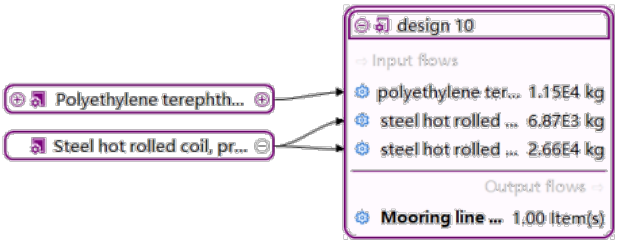

Figure 6: MATERIAL INPUT FLOWS FOR "DESIGN 10" OF SINGLE-SPAR PLATFORM CONCEPTS IN OPENLCA.

3.1 Mooring designs for single-spar platforms

For the single-spar platform, ten alternative mooring configurations ("Design 01" to "Design 10") are evaluated at water depths of 243.3 m and 799.2 m. The designs differ mainly in chain diameter, line length, and the corresponding mass of steel and polyester, while the overall three-segment layout of the mooring line remains unchanged. For each configuration, both studless and stud link chains are considered for Segments 1 and 3, whereas Segment 2 always uses polyester rope. The resulting design parameters are presented in Table 1.

Figure 7 presents the manufacturing cost of the complete mooring line (Segments 1 to 3) for different mooring configurations, chain types, and water depths. Clear and consistent trends are observed across both water depths considered. In all cases, the total manufacturing cost increases with increasing chain diameter and mooring line length, indicating a strong dependence on steel mass. Designs employing stud-link chains are systematically more expensive than their studless counterparts for the same geometric configuration, reflecting the higher mass per unit length associated with stud-link chains.

Segment 3 dominates the overall manufacturing cost due to its substantially greater length and steel mass compared to the other segments. Consequently, configurations with thicker chains or extended Segment 3 lengths exhibit the highest total cost. This dominance becomes more pronounced at greater water depths, where the required mooring line length increases significantly. For configurations incorporating polyester rope in Segment 2, the contribution of the rope to the total manufacturing cost is smaller than that of the steel chain segments. Nevertheless, its cost is not negligible, particularly in deep-water cases where rope length increases considerably. The results indicate that, while polyester rope does not control the total cost, its inclusion affects the overall balance between material usage and cost efficiency.

The lower and upper cost bounds shown in Figure 7 reflect the range of unit prices adopted in the LCC model and consistently bracket the reference cost values provided by

Table 1: DESIGN PARAMETERS OF MOORING LINES FOR A SINGLE-SPAR PLATFORM.

Design No.	Water depth: 243.3 m						Water depth: 799.2 m					
	Length [m]			Diameter [m]			Length [m]			Diameter [m]		
	Seg. 1	Seg. 2	Seg. 3	Seg. 1	Seg. 2	Seg. 3	Seg. 1	Seg. 2	Seg. 3	Seg. 1	Seg. 2	Seg. 3
Design 01	30.0	583.9	116.0	0.100	0.130	0.100	50.0	959.0	189.8	0.100	0.130	0.100
Design 02	30.0	583.9	116.0	0.100	0.130	0.100	50.0	959.0	189.8	0.100	0.130	0.100
Design 03	30.0	583.9	116.0	0.100	0.130	0.100	50.0	959.0	189.8	0.100	0.130	0.100
Design 04	30.0	681.2	140.3	0.100	0.130	0.100	50.0	959.0	189.8	0.110	0.130	0.110
Design 05	30.0	583.9	116.0	0.110	0.130	0.110	50.0	959.0	189.8	0.110	0.130	0.110
Design 06	30.0	681.2	140.3	0.100	0.130	0.100	50.0	959.0	189.8	0.110	0.130	0.110
Design 07	30.0	583.9	116.0	0.110	0.130	0.110	50.0	959.0	189.8	0.100	0.170	0.100
Design 08	30.0	681.2	140.3	0.100	0.130	0.100	50.0	1278.7	269.7	0.100	0.130	0.100
Design 09	30.0	583.9	116.0	0.110	0.130	0.110	50.0	959.0	189.8	0.100	0.170	0.100
Design 10	30.0	778.6	164.6	0.100	0.130	0.100	50.0	959.0	189.8	0.120	0.130	0.120

Table 2: DESIGN PARAMETERS OF MOORING LINES FOR A SINGLE-SEMI-SUBMERGED PLATFORM.

Design No.	Water depth: 243.3 m						Water depth: 799.2 m					
	Length [m]			Diameter [m]			Length [m]			Diameter [m]		
	Seg. 1	Seg. 2	Seg. 3	Seg. 1	Seg. 2	Seg. 3	Seg. 1	Seg. 2	Seg. 3	Seg. 1	Seg. 2	Seg. 3
Design 01	30.0	583.9	50.0	0.100	0.130	0.100	50.0	960.0	190.0	0.100	0.130	0.100
Design 02	30.0	583.9	50.0	0.102	0.130	0.102	50.0	960.0	190.0	0.102	0.130	0.102
Design 03	30.0	583.9	50.0	0.105	0.130	0.105	50.0	960.0	190.0	0.105	0.130	0.105
Design 04	30.0	583.9	50.0	0.107	0.130	0.107	50.0	960.0	190.0	0.107	0.130	0.107
Design 05	30.0	681.2	50.0	0.100	0.130	0.100	50.0	900.0	250.0	0.100	0.130	0.100
Design 06	30.0	583.9	50.0	0.100	0.170	0.100	50.0	960.0	190.0	0.111	0.170	0.111
Design 07	30.0	583.9	50.0	0.102	0.170	0.102	50.0	960.0	190.0	0.100	0.170	0.100
Design 08	30.0	583.9	50.0	0.105	0.170	0.105	50.0	960.0	190.0	0.102	0.170	0.102
Design 09	30.0	681.2	50.0	0.100	0.170	0.100	50.0	960.0	190.0	0.100	0.170	0.100
Design 10	30.0	583.9	50.0	0.100	0.130	0.100	50.0	960.0	190.0	0.102	0.170	0.102

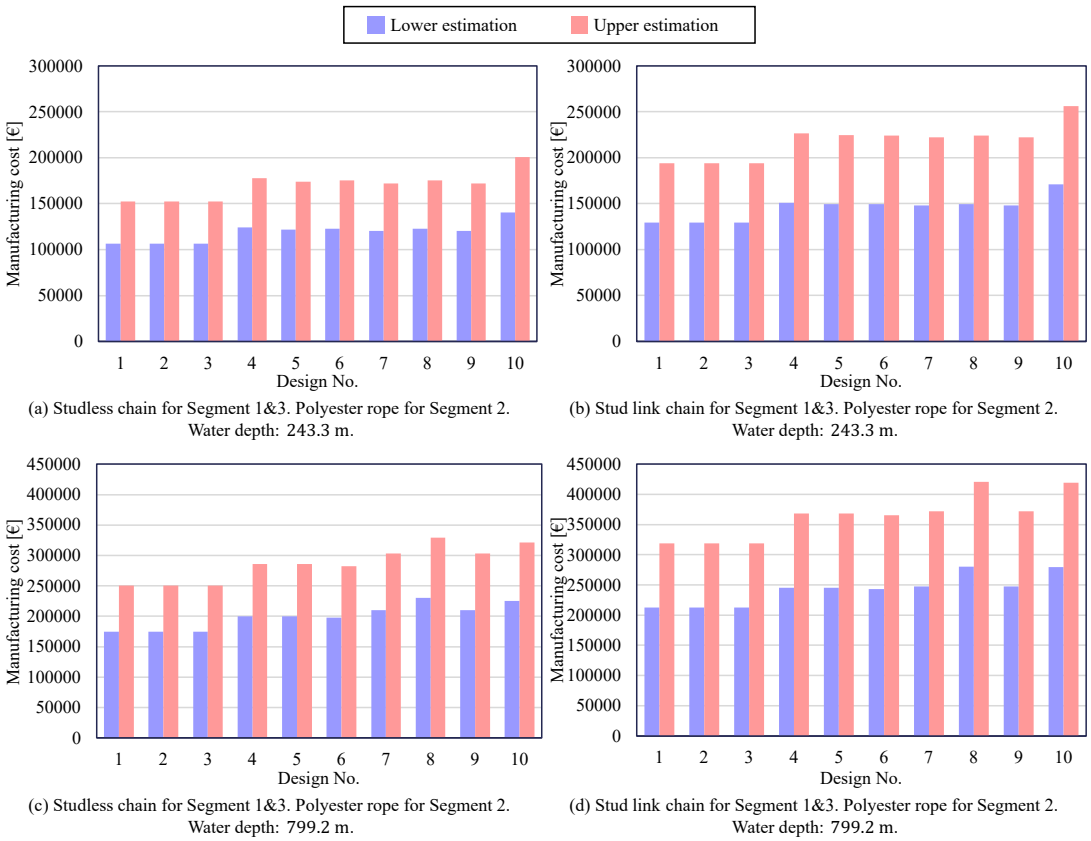

Figure 7: TOTAL COST OF MOORING LINES FOR A SINGLE-SPAR PLATFORM.

industrial partners. This agreement supports the plausibility of the adopted cost assumptions.

Figure 8 presents the CO_2 emissions associated with the manufacturing of one mooring line for each design. In all cases, the steel production for Segments 1 and 3 is the dominant contributor to total emissions, while the polyester rope in Segment 2 adds a smaller contribution due to its recycling process. This is reflected in Figure 8, where the "steel hot rolled coil" bars are much higher than the "polyethylene terephthalate (PET) granulate" bars for every design. As expected, designs that contain more steel, either due to larger chain diameters or longer lengths of Segment 3, show higher total CO_2 emissions. Similarly, the deep-water configurations (799.2 m) exhibit substantially higher emissions than the shallow-water configurations because of the increased line lengths and masses. Across all ten designs and both chain types, the total manufacturing-phase emissions per mooring line lie in the range of several tens of tonnes of CO_2 -equivalent, with stud-link configurations systematically above their studless counterparts.

Based on the combined LCC and LCA results presented in the case study, "Design 01" emerges as the most favorable configuration among the ten alternatives under the current assumptions. It consistently exhibits the lowest manufacturing cost and one of the lowest CO_2 emission levels. This design, therefore, will be selected for further studies.

3.2 Mooring designs for single-semi-submerged platforms

Using the same methodology applied in Section 3.1, another case study was conducted for a single semi-submerged platform. Ten mooring system configurations ("Design 01" to "Design 10" listed in Table 2) were evaluated following the same three-segment modelling approach and the same LCC and LCA procedures.

The total manufacturing cost of the complete mooring line (Segments 1 to 3) for both chain types and water depths is illustrated in Figure 9. The CO_2 emissions for each design, based on the manufacturing of one mooring line, are reported in Figure 10. Similar to the case study on the single-spar platform presented in Section 3.1, based on the resulting LCC and LCA outcomes, "Design 01" emerges as the most cost-efficient and environmentally favorable configuration among the evaluated alternatives under the current assumptions. Consequently, this design is selected as the recommended configuration for further analysis activities related to the semi-submerged platform.

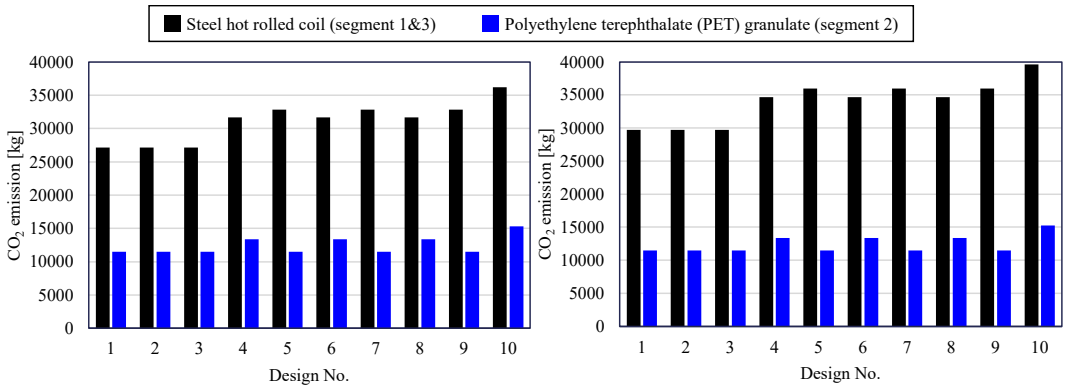

(a) Studless chain for Segment 1&3. Polyester rope for Segment 2. Water depth: 243.3 m.

(b) Stud link chain for Segment 1&3. Polyester rope for Segment 2. Water depth: 243.3 m.

(c) Studless chain for Segment 1&3. Polyester rope for Segment 2. Water depth: 799.2 m.

(d) Stud link chain for Segment 1&3. Polyester rope for Segment 2. Water depth: 799.2 m.

Figure 8: TOTAL CO_2 EMISSION OF MOORING LINES FOR A SINGLE-SPAR PLATFORM.

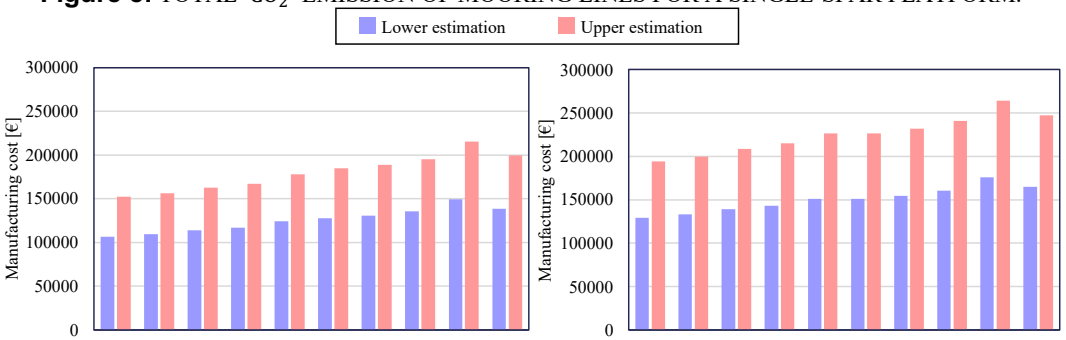

(a) Studless chain for Segment 1&3. Polyester rope for Segment 2. Water depth: 243.3 m.

(b) Stud link chain for Segment 1&3. Polyester rope for Segment 2. Water depth: 243.3 m.

(c) Studless chain for Segment 1&3. Polyester rope for Segment 2. Water depth: 799.2 m.

(d) Stud link chain for Segment 1&3. Polyester rope for Segment 2. Water depth: 799.2 m.

Figure 9: TOTAL COST OF MOORING LINES FOR A SINGLE-SEMI-SUBMERGED PLATFORM.

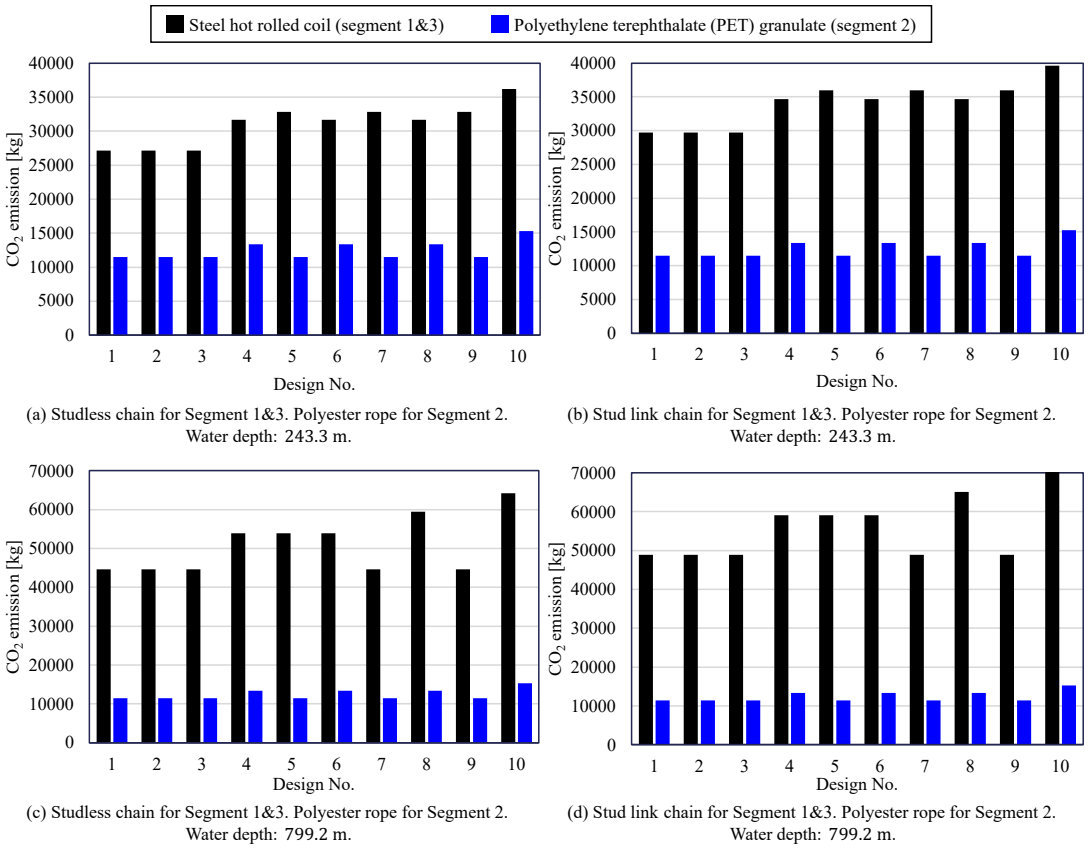

(a) Studless chain for Segment 1&3. Polyester rope for Segment 2. Water depth: 243.3 m.

(b) Stud link chain for Segment 1&3. Polyester rope for Segment 2. Water depth: 243.3 m.

(c) Studless chain for Segment 1&3. Polyester rope for Segment 2. Water depth: 799.2 m.

(d) Stud link chain for Segment 1&3. Polyester rope for Segment 2. Water depth: 799.2 m.

Figure 10: TOTAL CO_2 EMISSION OF MOORING LINES FOR A SINGLE-SEMI-SUBMERGED PLATFORM.

4. CONCLUSIONS

This study presented an integrated life-time engineering (LTE) framework for floating offshore wind farms that consistently combines life-cycle cost (LCC), life-cycle assessment (LCA), and life-cycle performance (LCP) considerations. The framework has been implemented in a modular computational environment in MATLAB and was demonstrated through two manufacturing-stage case studies focusing on mooring system design. The results show that mooring line configuration, material selection, and water depth have a strong influence on both cost and environmental impact, with steel mass being the dominant driver. By revealing coupled cost-environmental trade-offs that cannot be identified through isolated analyses, the proposed LTE framework provides a practical and extensible tool for early-stage design evaluation and supports informed decision-making for floating offshore wind development.

ACKNOWLEDGEMENTS

This work was carried out within the framework of the ESOMOOR project (Enhancing Shared mOoring systeM design for flOating Offshore wind faRms), which is funded by the European Union through the Clean Energy Transition Partnership (CETPartnership, project no. CETP-2023-00145).

REFERENCES

[1] Berg, K., Mattson, F., and Kochmann, M., "Floating Substations Joint Industry Project," Proc. Offshore Technology Conference, OTC, p. D021S021R007.

[2] Brown-Saracino, J., Sumait, N., Leibman, A., McKenzie, N., and Fu, J., 2024, "Floating Offshore Wind Shot: Priorities, Progress, and Next Steps," Floating Wind Solutions / DOE / BOEM.

[3] Alting, D. L., and Jøgensen, D. J., 1993, "The life cycle concept as a basis for sustainable industrial production," CIRP annals, 42(1), pp. 163-167.

[4] Penciuc, D., Le Duigou, J., Daaboul, J., Vallet, F., and Eynard, B., 2016, "Product life cycle management approach for integration of engineering design and life cycle engineering," AI EDAM, 30(4), pp. 379-389.

[5] Saincher, S., Sriram, V., and Stoesser, T., 2025, "Shared moorings for floating offshore renewable energy technologies: A review," Renewable and Sustainable Energy Reviews, 224, p. 116064.

[6] ISO, 2006, "ISO 14044:2006 - Life Cycle Assessment."

[7] Chemineau, M., Castillo, F., Mechinaud, L., Arramounet, V., and Gilloteaux, J., "Design and costs benefits of shared anchors and shared mooring lines of floating wind turbines at farm level," Proc. Journal of Physics: Conference Series, IOP Publishing, p. 012048.

[8] Paduano, B., 2026, "Current status and perspectives on shared moorings for offshore floating renewable energy systems: A review," Renewable and Sustainable Energy Reviews, 226, p. 116350.

[9] Pan, Q., Liu, D., Guo, F., and Cheng, P. W., 2024, "A Comprehensive Design Methodology of Shared Mooring Line Configurations for Assessing Mooring Costs and Performances of

Floating Offshore Wind Turbines," Wind Energy Science Discussions, 2024, pp. 1-32.

[10] Striani, R., Jiang, H., Biroli, M. V., Shao, Y., and Wang, S., 2025, "Review of Floating Offshore Wind Turbines with Shared Mooring Systems," Journal of Marine Science and Engineering, 13(12), p. 2341.

[11] Timmington, D., and Efthimiou, L., 2022, "Mooring Systems for Floating Offshore Wind: Integrity Management Concepts, Risks and Mitigation."

[12] Xu, H., Rui, S., Shen, K., Jiang, L., Zhang, H., and Teng, L., 2024, "Shared mooring systems for offshore floating wind farms: A review," Energy Reviews, 3(1), p. 100063.

[13] Falkenberg, E., Yang, L., and Åhjem, V., "Spring-dashpot simulations of polyester ropes: validation of the syrope model," Proc. International Conference on Offshore Mechanics and Arctic Engineering, American Society of Mechanical Engineers, p. V001T001A050.

[14] Castro-Santos, L., Filgueira-Vizoso, A., Carral-Couce, L., and Formoso, J. Á. F., 2016, "Economic feasibility of floating offshore wind farms," Energy, 112, pp. 868-882.

[15] Castro-Santos, L., Martins, E., and Guedes Soares, C., 2016, "Methodology to calculate the costs of a floating offshore renewable energy farm," Energies, 9(5), p. 324.

[16] Castro-Santos, L., Martins, E., and Soares, C. G., 2016, "Cost assessment methodology for combined wind and wave floating offshore renewable energy systems," Renewable energy, 97, pp. 866-880.

[17] Garcia-Teruel, A., Rinaldi, G., Thies, P. R., Johanning, L., and Jeffrey, H., 2022, "Life cycle assessment of floating offshore wind farms: An evaluation of operation and maintenance," Applied Energy, 307, p. 118067.

[18] Di Noi, C., Ciroth, A., and Srocka, M., 2017, "OpenLCA 1.7," Comprehensive User Manual, GreenDelta GmbH, Berlin, Germany.

[19] Guinée, J. B., 2002, Handbook on life cycle assessment: operational guide to the ISO standards, Springer Science & Business Media.

[20] Thöns, S., Faber, M. H., and Rücker, W., 2012, "Fatigue and serviceability limit state model basis for assessment of offshore wind energy converters."

[21] Long, H., and Moe, G., 2012, "Preliminary design of bottom-fixed lattice offshore wind turbine towers in the fatigue limit state by the frequency domain method."

[22] Thöns, S., Faber, M. H., and Rücker, W., 2012, "Ultimate limit state model basis for assessment of offshore wind energy converters."

[23] Paik, J. K., Kim, B. J., and Seo, J. K., 2008, "Methods for ultimate limit state assessment of ships and ship-shaped offshore structures: Part I—Unstiffened plates," Ocean Engineering, 35(2), pp. 261-270.

[24] Paik, J., and Thayamballi, A., 2006, "Some recent developments on ultimate limit state design technology for ships and offshore structures," Ships and Offshore Structures, 1(2), pp. 99-116.

[25] Benassai, G., Campanile, A., Piscopo, V., and Scamardella, A., 2014, "Ultimate and accidental limit state design for mooring systems of floating offshore wind turbines," Ocean Engineering, 92, pp. 64-74.

[26] Striani, R., Biroli, M., and Wang, S., 2025, "ESOMOOR D3.1: Definition of two floaters for IEA 15WM turbine for at least two water depths in Europe and the US.."

[27] Wei, Z. S., Yanlin; Bingham, Harry B., 2025, "ESOMOOR D3.2b: Design basis and technology gap analysis report."

[28] Depalo, F., Wang, S., Xu, S., and Guedes Soares, C., 2021, "Design and analysis of a mooring system for a wave energy converter," Journal of Marine Science and Engineering, 9(7), p. 782.

[29] DNV, 2018, "Offshore standards DNV-OS-E301: Position mooring."

[30] Nunemaker, J., Shields, M., Hammond, R., and Duffy, P., 2020, "ORBIT: Offshore renewables balance-of-system and installation tool," National Renewable Energy Lab.(NREL), Golden, CO (United States).